Available online at www.sciencedirect.com

Catalysis Today 99 (2005) 105–114

www.elsevier.com/locate/cattod

Comparison of alcohol and alkane oxidative dehydrogenation reactions over supported vanadium oxide catalysts: in situ infrared, Raman and UV–vis spectroscopic studies of surface alkoxide intermediates and of their surface chemistry

Carlo Resini[a,c], Tania Montanari[a], Guido Busca[a,*], Jih-Mirn Jehng[b,c], Israel E. Wachs[c]

[a]*Laboratorio di Chimica delle Superfici e Catalisi Industriale, Dipartimento di Ingegneria Chimica e di Processo, Università di Genova, P.le Kennedy, I-16129 Genova, Italy*
[b]*Department of Chemical Engineering, National Chung Hsing University, 250 Kuokuang Road, Taichung 402, Taiwan, PR China*
[c]*Operando Molecular Spectroscopy and Catalysis Laboratory, Department of Chemical Engineering, Lehigh University, 7 Asa Drive, Bethlehem, PA 18015, USA*

Available online 17 January 2005

Abstract

The surface chemistry of adsorbed isopropoxy groups on supported vanadia–alumina and vanadia–silica catalysts was investigated with multiple in situ spectroscopic techniques. The in situ FT-IR, Raman and UV–vis spectroscopic measurements provided molecular level information about the surface intermediates and the surface vanadium oxide species as a function of different conditions. The spectroscopic insights were compared to the steady state fixed bed catalytic reaction studies of isopropanol oxidation and propane oxidative dehydrogenation in order to better understand the molecular structure–reactivity/selectivity relationships.

Keywords: Isopropoxy group; UV–vis spectroscopic measurement; Surface vanadium oxide species; FT-IR spectroscopy; Raman spectroscopy; Oxidative dehydrogenation

1. Introduction

Heterogeneously catalyzed selective oxidations represent a wide family of key processes in petrochemistry [1]: they occur through a sequence of a number of different phenomena such as reactants gas-phase and intrapore diffusion, adsorption, surface reactions, products desorption and diffusion [2]. Also the chemical features are frequently constituted by a sequence of several surface phenomena, different reaction steps and desorption/adsorption of intermediates. For these reasons, mechanistic studies and studies of the active surface sites [3–6] are needed to attempt improvement of catalytic performances. The detection by spectroscopy of the surface intermediates, when possible, allows the development of ‘‘the surface science of catalytic activity/selectivity’’ [7].

For the past five decades, in situ IR spectroscopy has been applied to detect species at the surfaces of the catalysts [8]. The surface species detected are not necessarily the active surface intermediates since the detection of spectators and/or poisons may sometimes be easier than that of active surface intermediates [9]. For the past two and half decades, Raman spectroscopy has been widely applied to the surface chemistry of oxide catalysts [10–12]. However, application of Raman spectroscopy to the investigation of surface intermediates or adsorbed species has been rather limited, and rarely are there combined IR and Raman spectroscopy studies in the literature [13]. Even more so for combined optical spectroscopy studies employing IR, Raman and UV–vis, especially in situ studies [13].

The conversion of isopropanol in the absence of oxygen is used widely as a chemical probe reaction [14]. In the

---

[*] Corresponding author. Tel.: +39 010 353 6024; fax: +39 010 353 6028.
E-mail address: Guido.Busca@unige.it (G. Busca).

0920-5861/$ – see front matter © 2004 Elsevier B.V. All rights reserved.
doi:10.1016/j.cattod.2004.09.029

absence of oxygen the selectivity in the conversion of isopropanol into propene by dehydration and acetone by dehydrogenation has been employed to determine the balance between surface acidity and basicity [15]. The extent of isopropanol oxidative dehydrogenation to acetone in the presence of oxygen is a measure of the surface redox potential of the catalyst or of its activity as a selective oxidation catalyst [16,17]. Several research groups [1,18,19] have proposed that surface alkoxide species are also reaction intermediates in selective oxidative dehydrogenation of the corresponding alkane [20].

In the present paper we report on combined in situ IR, Raman and UV–vis spectroscopic studies of the catalytic conversion of isopropanol in the presence of oxygen over two oxide-supported vanadia catalysts: V_2O_5/Al_2O_3 and V_2O_5/SiO_2. Such fundamental studies can provide additional insights about the surface reaction mechanism of the oxidative dehydrogenation of propane because of their proposed common reaction intermediates and reaction products, as well as other alkanes, over supported vanadia catalysts.

2. Experimental

2.1. Catalysts preparation

The V_2O_5-supported on Al_2O_3 (Harshaw, ~210 m^2/g), and SiO_2 (Cab-O-Sil, EH-5, ~320 m^2/g) catalysts were prepared by the incipient-wetness impregnation method in order to obtain supported 20% V_2O_5/Al_2O_3 and supported 10% V_2O_5/SiO_2 samples (hereinafter denoted as 20VA and 10VS), respectively. These surface vanadia concentration correspond to ~80% and ~70% monolayer surface vanadia coverage on the Al_2O_3 and SiO_2 support, respectively. The SiO_2 support was pretreated with water and calcined at 773 K for 16 h under flowing dry air in order to condense its volume. The water pretreatment has no effect on the BET surface area of the silica support. Vanadium isopropoxide (Alfa, 95–99% purity) in a propanol solution (Fisher, 99.9% purity) was impregnated into the oxide supports by using the non-aqueous preparation procedure under a nitrogen environment (incipient-wetness impregnation). The samples were initially dried at room temperature for 2 h to remove excess propanol and further dried at 393 K for 16 h under flowing N_2. The samples were finally calcined at 773 K for 1 h under flowing N_2, and for an additional 1 h under flowing dry air.

2.2. FT-IR spectroscopy

The IR spectra were recorded on a Nicolet Protégé Fourier Transform instrument, using pressed disks of pure sample powders (15 mg for 2 cm diameter), and activated by outgassing at 623 K. A conventional gas manipulation/outgassing ramp connected to the IR cell was used. The adsorption procedure involves contact of the activated sample disk with isopropanol vapors (50 Torr). The gas–solid systems were initially equilibrated for 10 min and then the spectra of the gas phase and of the sample surface were recorded. The cell was subsequently evacuated and left under static vacuum for 10 min in order to allow the physisorbed gas to evolve from the catalyst surface. Both the gas phase and the sample spectra were recorded before evacuating the cell. The same procedure has been repeated at increasing temperatures (from RT up to 773 K in increments of 100 K)

2.3. In situ Raman spectroscopy

The in situ Raman spectrometer system consists of a quartz cell with a sample holder, a triple-grating spectrometer (Spex, Model 1877), a CCD detector (Jobin Yvon-Spex, ISA Inc., Model Spectrum-1) and an argon ion laser ($\lambda = 514.5$ nm) (Spectra-Physics, Model 165). The sample holder is made from a metal alloy (Hastalloy C), and a 100–200 mg sample disc is held by the cap of the sample holder. The sample holder is mounted onto a ceramic shaft which is rotated by a 115 V dc motor at a speed of 1000–2000 rpm. A cylindrical heating coil surrounding the quartz cell is used to heat the cell. The quartz cell is capable of operating up to 873 K, and flowing gas is introduced into the cell at a rate of 100–200 cc/min at atmospheric pressure.

The in situ Raman spectra were obtained by the following procedures. The samples were placed into the cell and heated up to 773 K for 1 h in flowing oxygen gas and the Raman spectrum was recorded. The dehydrated Raman spectrum was collected after cooling the sample to 573 K in a flow of pure oxygen gas for 30 min. After the above treatment, a flowing 1:4 $C_3H_7OH:O_2$ in He gaseous mixture was introduced into the cell, and the Raman spectra under reaction temperature between RT and 773 K were collected after reaching steady state at each temperature. Finally, the Raman spectra of the reoxidized samples at 773 K under flowing oxygen were recorded.

2.4. DR UV–vis spectroscopy

Diffuse reflectance UV–vis spectra in the range 4000–50,000 cm^{-1} were recorded in a *Jasco* V-570 UV–vis–NIR spectrophotometer. The UV–vis spectra were measured after exposing the samples to vacuum outgassing and to isopropanol at different temperatures.

The in situ UV–vis DRS spectra of the supported vanadia catalysts under different environmental flowing conditions were recorded in a Varian Cary 5E UV–vis–NIR spectrophotometer after initially calcining samples at 773 K in flowing O_2/He for 1 h.

2.5. Catalytic tests

The catalytic experiments were carried out in a fixed-bed tubular quartz reactor connected to a GC (Agilent 5890) equipped with a PORAPLOT Q (HP) capillary column, which was connected to a TCD detector in series with a FID detector. A nickel catalyst tube between the TCD and FID detectors was employed to reduce the CO to CH_4. A six-port valve with a 0.5 cm^3 loop was used for the gas sampling of the outlet gases. The reactant feed gas mixture had the following composition: 13% isopropanol and 2% O_2 in helium with a total flow of 100 ml/min.

3. Results

3.1. Catalytic experiments

The conversion/selectivities versus temperature trends for isopropanol oxidation of the supported 20VA sample catalyst are shown in Fig. 1. The reaction initiates above 400 K and reaches complete conversion of isopropanol at 523 K. The maximum oxygen conversion asymptotically approaches 18% at 573 K. The main reaction products are acetone and propylene with small amounts of di-isopropyl ether. Acetone is the major reaction product at low conversions and temperatures (60% selectivity at 423 K), and its selectivity decreases with increasing temperature (60% at 423 K to 5% at 573 K). The corresponding propylene selectivity increases with increasing temperature (from 25% at 423 K to 92% at 573 K). Di-isopropyl ether was only detected at low reaction temperatures (15% of selectivity at 423 K) and only trace amounts of CO_x were formed.

A similar series of isopropanol oxidation reaction studies were performed over the 10VS sample. The conversion/selectivity versus temperature trends are presented in Fig. 2 and demonstrate that the reaction starts above 400 K. The conversion of isopropanol reaches 100% at 573 K and the oxygen conversion exceeds 10% at 623 K. The acetone selectivity is 35% at 423 K and decreases with increasing temperature, and levels out at 5% at 623 K. In contrast, the propylene selectivity is much higher than the acetone selectivity and increases with temperature (from 52% at 423 K up to 92% at 573 K). Only minor amounts of di-isopropyl ether were formed (at 423 K with a selectivity of 8%) and CO_x was detected in trace amounts only at the lowest reaction temperature (373 K).

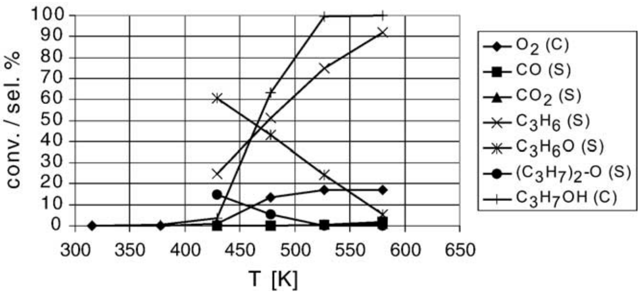

Fig. 1. Conversion/selectivity (%) vs. temperature trends of isopropanol over 20VA.

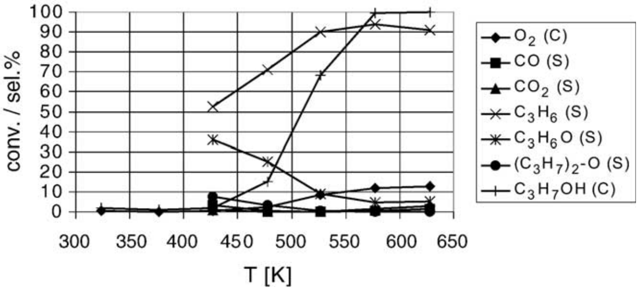

Fig. 2. Conversion/selectivity (%) vs. temperature trends of isopropanol over 10VS.

3.2. In situ IR and Raman spectroscopic study

Supported vanadia alumina: The in situ IR spectrum of the supported 20VA catalyst, after initial evacuation in vacuum at 623 K and subsequent isopropanol adsorption at RT, are shown as a function of different heating temperatures in Fig. 3. The spectra exhibit a broad absorption band in the 3750–3500 cm^{-1} region due to the surface hydroxy groups, and a strong band at 1045 cm^{-1} previously assigned to the terminal V=O stretching of surface vanadyl groups (see Fig. 4a) [11,21]. Fig. 4 shows the spectra resulting from the subtraction of the spectrum of the activated sample from the spectrum of the sample with the adsorbed species. The overtone of the V=O stretching band can be detected as a weak band at 2050 cm^{-1} (see Fig. 4b). Absorptions are also observed at 1550 and 1450 cm^{-1} (see Fig. 3), which originates from surface carboxylate species present on the catalyst surface.

Isopropanol adsorption results in the appearance of C–H stretching bands in the 3000–2700 cm^{-1} region at 2974, 2935, 2899 and 2878 cm^{-1} (see Fig. 3). The corresponding deformation IR bands appear in Fig. 4a and are assigned as follows: the asymmetric CH_3 deformation bands at 1465 and 1454 cm^{-1}, the symmetric CH_3 deformation doublet (typical of isopropyl species) at 1383 and 1369 cm^{-1}, and the $CH(CH_3)$ deformation band at 1330 cm^{-1}. The appearance of a broad band at ~1280 cm^{-1} arises from the OH deformation mode of undissociated, adsorbed isopropanol [22], and decreases with increasing the temperature (see Fig. 4a). This indicates that the remaining C–H stretching and deformation bands are due to surface isopropoxy species. In agreement with this, strong IR bands are also present at 1105 cm^{-1}, with a shoulder at 1130 cm^{-1}, and a smaller band at 1166 cm^{-1} that arise from coupled C–O/C–C stretchings of the surface isopropoxy species (see Fig. 4a).

The background subtracted IR spectra more clearly reveal the shift of the V=O band of the surface vanadyl species from 1045 (negative band in the subtracted spectra) to 1006 cm^{-1} (positive band) (see Fig. 4a) and of the corresponding first overtone from 2050 to 2014 cm^{-1} (see Fig. 4b) in the presence of adsorbed isopropanol due interaction of the surface isopropoxide species with the

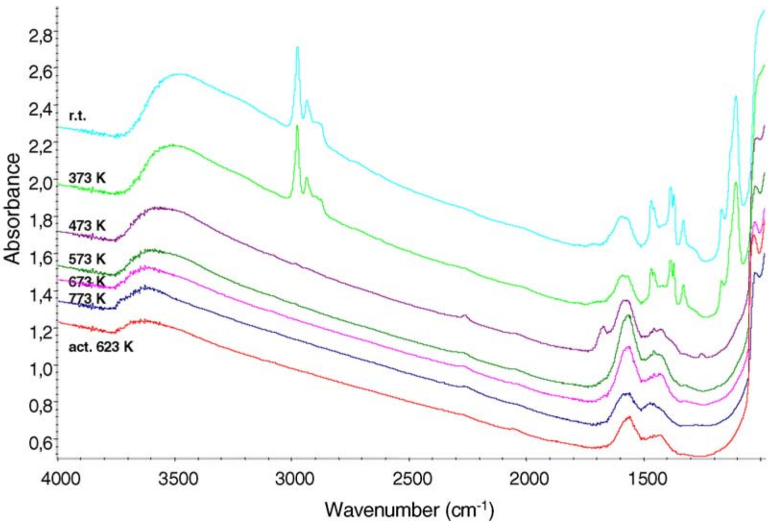

Fig. 3. In situ FT-IR spectra of isopropanol adsorption on 20VA experiment.

surface vanadia sites. Heating to 473 K causes the complete disappearance of the bands of surface isopropoxide species with the appearance of new bands at 1680 cm^{-1} and at 1240 cm^{-1} due to the C=O stretching and the C–C–C asymmetric stretching of adsorbed acetone (see Fig. 4a) [23]. These adsorbed acetone bands also disappear after reaching 573 K when the bands of surface carboxylate species, already present in the spectrum of the starting activated catalyst, are perhaps slightly increased in intensity.

The Raman spectra of the supported 20VA catalyst under different environmental conditions are presented in the 1300–400 cm^{-1} region in Fig. 5. No Raman vibrations due to C–H vibrations were detected above 1100 cm^{-1}. Under flowing O_2/He a pronounced band is observed at ~1030–1028 cm^{-1}, due to the terminal V=O stretching mode of the surface vanadyl species [10–13]. The broad Raman bands at 770 and 535 cm^{-1} correspond to the symmetric and asymmetric stretches of the bridging V–O–V bonds. The detection of the bridging V–O–V bonds reveals that the presence of polymeric surface vanadia species for the dehydrated supported 20% V_2O_5/Al_2O_3 catalyst [10,12,13]. The small band at 994 cm^{-1} corresponds to trace quantities of crystalline V_2O_5 due to its strong Raman cross-section [12]. Upon exposure to isopropanol/He at RT, a broad band appears at 940 cm^{-1} assignable to V–O–V or V–O–Al stretching vibrations, and the terminal V=O vibrations shift from 1030 to 1015 cm^{-1} due to interaction of the surface vanadia species with the adsorbed isopropanol. Sharper bands at 994, 702 and 530 cm^{-1} are also present at RT due to the trace of crystalline V_2O_5 [12]. The 994 cm^{-1} band corresponds to the V=O stretching vibration, and the 702 and 530 cm^{-1} bands correspond to the asymmetric and symmetric stretches of the bridging V–O–V functionality [12]. The Raman bands at 535 and 770 cm^{-1} originate from the symmetric and asymmetric vibration of bridging V–O–V bands. No bands assignable to C–H stretching and deformation modes are detected in the 3000–2700 cm^{-1} region (see Fig. 5). Upon heating to higher temperature, the Raman spectrum of the initially dehydrated supported vanadia–alumina catalyst is progressively restored. The surface vanadyl stretching sharpens and shifts progressively towards the original position at 1030 cm^{-1} with increasing

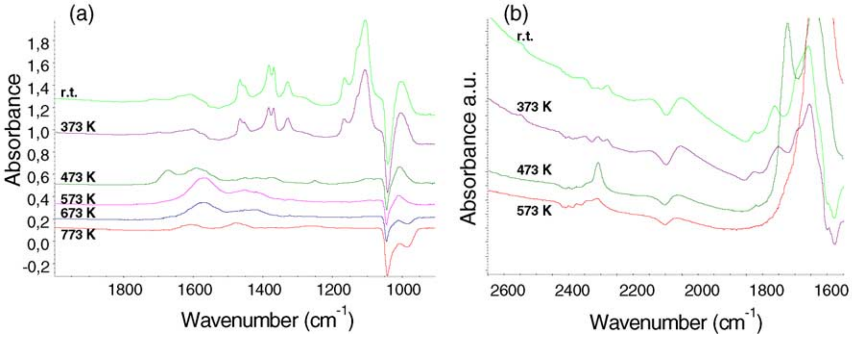

Fig. 4. In situ FT-IR spectra of isopropanol adsorption on 20VA experiment: subtraction spectra (a) C–H deformations and vanadyl stretching; (b) vanadyl overtone.

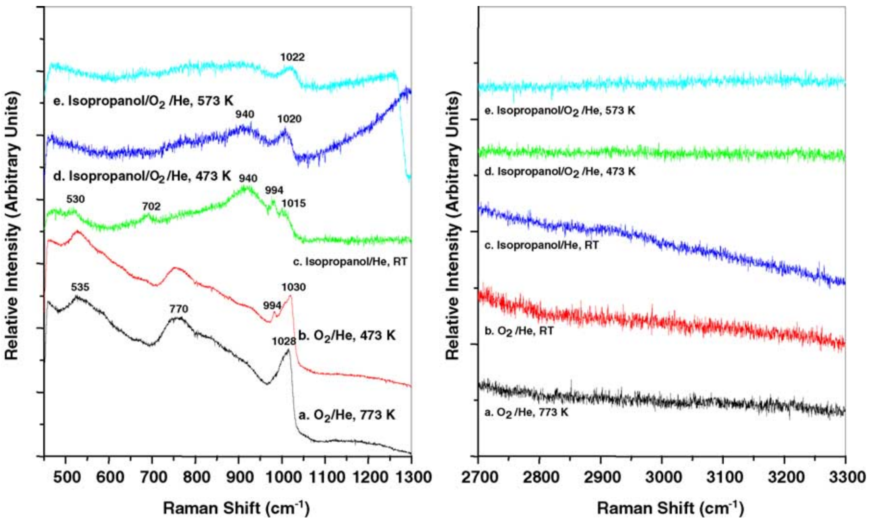

Fig. 5. In situ Raman spectra of isopropanol adsorption on 10VS experiment.

temperature during isopropanol oxidation. These shifts are related to decreased interactions of the surface V=O bond with surface concentration of the reaction intermediates and adsorbed moisture as their surface concentrations decrease with temperature (see Figs. 3–5).

Supported vanadia silica: The IR spectrum of the supported 10VS catalyst after activation in vacuum at 623 K is shown at the bottom of Fig. 6 and exhibits a sharp band at 3745 cm^{-1} due to the free silanol groups and weaker bands in the region 3730–3450 cm^{-1} region due to H-bonded hydroxy silanol groups. The broad triplet bands in the region 2050–1500 cm^{-1} region originate from the harmonics of the bulk skeletal absorptions of the silica support. The SiO_2 absorption becomes very strong below 1300 cm^{-1} due these absorptions and results in the IR spectral cut-off limit. A very weak feature in the range 2055–2016 cm^{-1} arises from the overtone of the terminal V=O stretching mode of the surface vanadyl groups on SiO_2 is also observed in Fig. 7b. Figs. 7 and 8 show the spectra resulting from the subtraction of the spectrum of the activated sample from the spectrum of the sample with the adsorbed species. The RT adsorption of isopropanol results in the formation of CH stretching bands at 2980, 2974, 2933, 2988, 2871 cm^{-1} (Fig. 7a), the asymmetric CH_3 deformation bands 1465 and 1454 cm^{-1}, of the symmetric CH_3 deformation doublet (typical of isopropyl species) at 1382 and 1369 cm^{-1}, and of the CH deformation band at 1329 cm^{-1} (Fig. 8). The OH deformation mode of molecularly adsorbed isopropanol in the range 1400–1200 cm^{-1} is not present and indicates that only surface isopropoxide species are present. The presence of surface isopropoxide is further supported by the strong and sharp band at 965 cm^{-1} assignable to coupled C–O/C–C

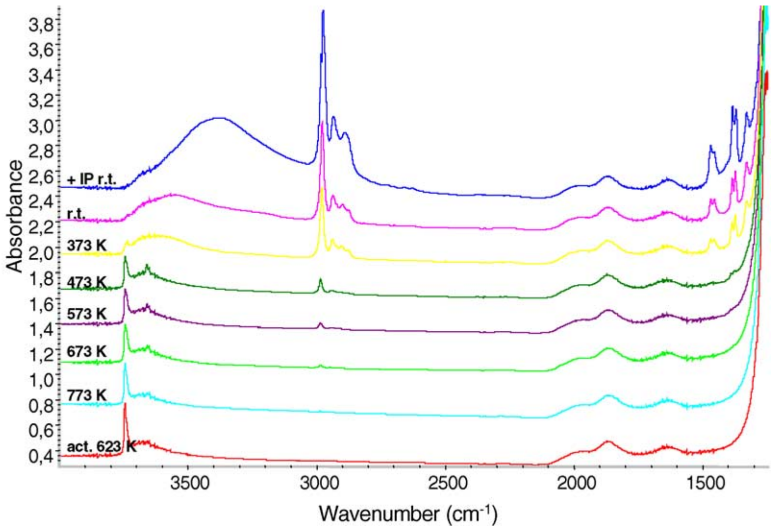

Fig. 6. In situ FT-IR spectra of isopropanol adsorption on 10VS experiment: subtraction spectra (a) OH and CH stretchings; (b) vanadyl overtone.

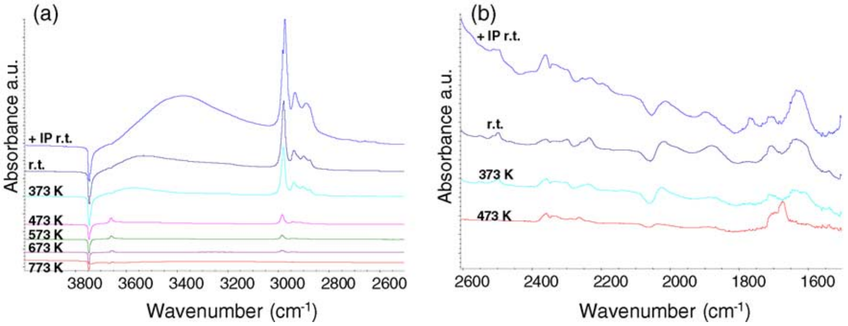

Fig. 7. In situ FT-IR spectra of isopropanol adsorption on 10VS experiment: subtraction spectra.

modes of the surface alkoxy species (see Fig. 8). All the surface isopropoxy IR bands strongly decrease in intensity by heating to 473 K, and almost disappear at higher temperatures without the appearance of new bands. A parallel study performed on pure silica suggests that these features are related to the presence of the surface vanadium oxide species. The small, sharp band at ~3650 cm^{-1} at 473–673 K has been previously assigned to the OH stretchings of VOH groups [24].

The corresponding Raman supported spectrum of the 10VS catalyst in flowing O_2/He at 773 K presented in Fig. 9 only exhibits one strong band at 1027 cm^{-1} due to the terminal V=O stretch of surface vanadyl species [12]. The absence of bridging V–O–V vibrations reflects the isolated nature of the surface vanadia species which are detected on SiO_2 support and the lack of crystalline V_2O_5 and of polyvanadate bands indicates that that the vanadia species are highly dispersed on the SiO_2 support in the case of this particular catalyst. Upon isopropanol adsorption at RT, the vanadyl band weakens slightly and shifts to 1012 cm^{-1} due to its interaction with surface isopropoxide. A new and strong Raman band is also observed at 965 cm^{-1} originating from the C–O/C–C stretching of the surface isopropoxide species, as well as weaker features at 1110 and 1162 cm^{-1} due to C–C/C–O coupled stretching of surface isopropoxy species. The weaker Raman bands at ~846, 775, 662 and 610 cm^{-1} are associated with the symmetric and asymmetric vibrations of the bridging V–O–C bonds between the surface isopropoxide species and the surface vanadia sites. Corresponding strong Raman bands are also observed in the CH stretching region at 2968 and 2926 cm^{-1}, weaker bands at 2910, 2895, and 2866 cm^{-1}, and very weak bands at 2720 and 2752 cm^{-1}. These Raman bands are associated with surface isopropoxide species and progressively decrease in intensity upon heating the catalyst. The surface isoproxide Raman bands completely disappear at 673 K, which indicates that no appreciable surface isopropoxide species remain at this and higher temperatures. The absence of the surface isopropoxide species at elevated temperatures also restores the initial terminal V=O vibration at 1032 cm^{-1} of the surface vanadia species.

3.3. In situ UV–vis–NIR spectroscopic study

The in situ UV–vis–NIR spectra of the catalysts supported vanadium oxide catalysts exhibit strong bands between 200 and 300 nm originating from $O^{2-} \rightarrow V^{5+}$ charge transfer transitions of low coordinated V^{5+} centers according to previous assignments [10–12,25–27]. The UV–vis spectra recorded in a cell allowing outgassing and contact with gases and vapors are presented in Fig. 10, and the conditions employed correspond to those used in the IR

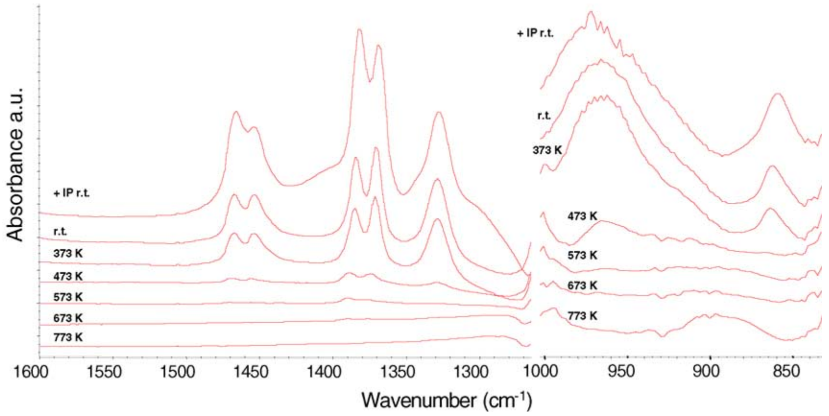

Fig. 8. In situ Raman spectra of isopropanol adsorption and reaction under flowing conditions over 20VA (C_3H_7OH:O_2 = 1:4).

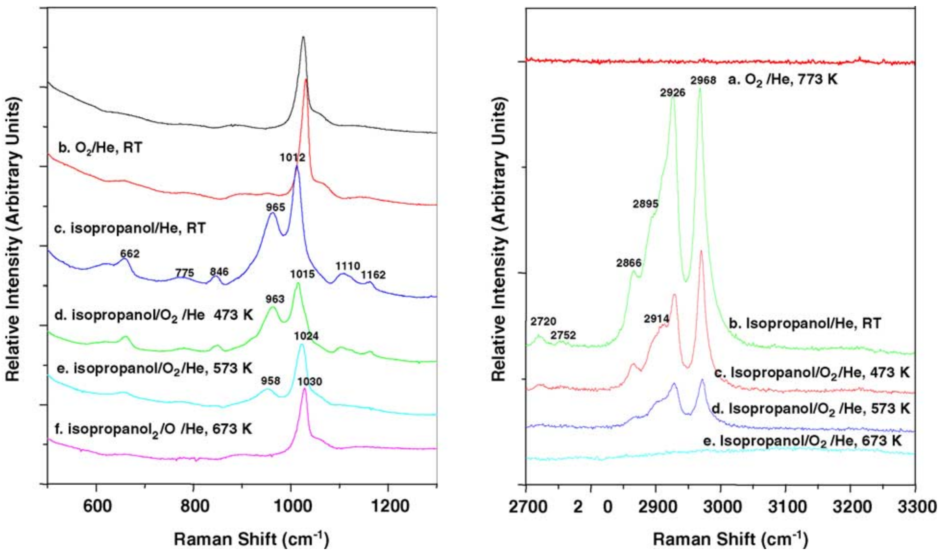

Fig. 9. In situ Raman spectra of isopropanol adsorption and reaction under flowing conditions over 10VS (C_3H_7OH:O_2 = 1:4).

spectroscopy measurements. After vacuum outgassing at room temperature, the spectrum of the supported vanadia alumina shows an absorption onset of 18000 cm^{-1}. Outgassing at higher temperatures causes a quite complete change in the spectrum, with the appearance of a broad continuous absorption in the overall visible region and the sample has a brown–black color. A similar effect is observed for vanadia–silica where the absorption onset occurs near 16000 cm^{-1} after outgassing at RT, and the sample strongly absorbs the visible light after outgassing at higher temperatures. Adsorption of isopropanol results in an even stronger absorption of visible and UV light. The almost continuous absorption in the visible region is reflects the reduction of V^{5+} to low oxidation state under these reducing vacuum conditions.

The UV–vis spectra were also recorded under different environmental conditions, employing flowing gases, as previously used for the Raman spectroscopy studies. The in situ UV–vis spectra of the two supported vanadia catalysts are recorded after treatment at 773 K in flowing O_2/He after 1 h are presented in Fig. 11. Under these environmental conditions, the surface vanadia species are fully oxidized and dehydrated [12]. The absence of the strong absorption extending to most of the IR region previously observed under evacuated conditions confirms that those strong absorptions indeed originate from reduced species produced by outgassing. The edge due to CT transitions of V^{5+} is a little lower in energy for VS (25000 cm^{-1}) than for VA (22,000 cm^{-1}) and the corresponding band gap energies (E_g) are 3.4 and 2.8 eV, respectively. The higher E_g value for the dehydrated 10VS and its slightly lower cut-off energy reflects the presence of only isolated surface vanadia species on the dehydrated SiO_2 surface [28,29]. The corresponding lower E_g value and higher energy for dehydrated 20VA reflects the presence of polymerized surface VO_4 species as well as isolated VO_4 units on the dehydrated Al_2O_3 surface [28,29]. Furthermore, during propane ODH the surface vanadia species were found to partially reduce, but the surface vanadia species were more extensively reduced on the Al_2O_3 (32–76%) support than on the SiO_2 support (2–12%) under comparable conditions as determined from the intensity decreases of the UV–vis bands.

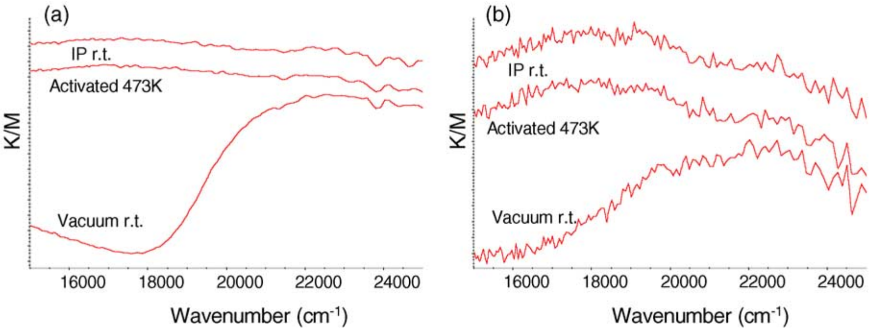

Fig. 10. In situ DR UV–vis–NIR of 20VA (a) and 10VS (b) spectra recorded in vacuum at RT, vacuum dehydrated at 473 K and with isopropanol adsorbed.

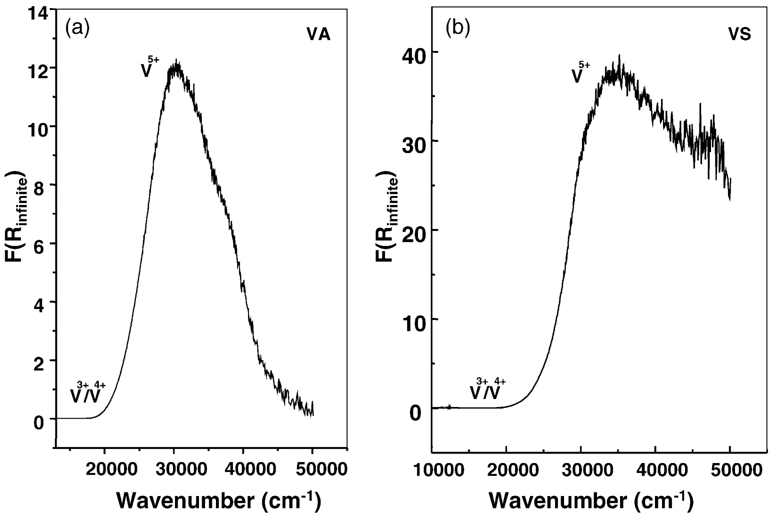

Fig. 11. In situ DR UV–vis–NIR of dehydrated and VA (a) VS (b) spectra.

4. Discussion

The surface vanadia species in the 10VSi and 20VAl samples appear to be highly dispersed since only trace quantities of crystalline V_2O_5 are detected. The surface vanadia species possess VO_4 coordination under dehydrated conditions, with one terminal V=O bond and three bridging V–O–M bonds, detected by IR and Raman spectroscopy [13,21,30–32]. Multiple vibrations would be expected for dioxo surface vanadium oxide species in the overtone region [21]. The in situ Raman and UV–vis spectroscopy studies revealed all the surface vanadia species are fully oxidized and dehydrated upon exposure to elevated temperatures and flowing O_2/He gases. The in situ UV–vis spectroscopy studies also demonstrated that dehydration under vacuum at elevated temperatures results in partially reduced surface vanadia species. These different dehydration procedures result in different degrees of surface hydration and reduction and are responsible for the slight vanadyl shift between the Raman and the IR of the surface vanadyl vibrations observed in this investigation. In situ IR measurements under flowing O_2/He confirm that the exact same bands are indeed obtained with Raman and IR for the terminal V=O vibrations of comparably dehydrated surface vanadyl species [13].

Exposure of the supported vanadia catalysts to isopropanol/O_2 results in the appearance of vibrations originating from surface isopropoxide species in the in situ IR and Raman spectra. Isopropoxides in their highest symmetry conformation can assume the point group Cs. They are expected to have 27 vibrational modes, 15 a′ and 12 a″, and all of them are IR and Raman active. The corresponding vibrational assignments of the surface isopropoxide species are shown in Table 1. The analysis of the intensity ratios between CH stretching and deformation vibrations reveals that these regions are far higher on VA than on VS. Surprisingly, Raman spectroscopy did not detect any band of surface isopropoxide vibrations for VAl. The observations indicate that the chemical bonding of the surface isopropoxide species with the surface vanadia species is significantly different in the two cases, and possibly its geometry may be different. It seems possible to suggest, in accordance with what has been previously reported for surface methoxides [11,12], that alkoxides on VA are more ionic and their CO possibly perpendicular to the surface while those on VS are more covalent and possibly bent. The lack of detection of most of the internal vibrations of isopropoxide species by Raman on VAl may also be due to these different characteristics. This is now the object of more detailed Raman and IR studies to better understand the origin of this different vibrational behavior.

The surface isopropoxide species are very reactive and significantly decompose between 373 and 473 K on both the supported VA and VS catalysts (see IR spectra in Figs. 3 and 6). The steady state isopropanol oxidation initiates at ~430 K on both supported VA and VS catalysts and is consistent with the decomposition of the surface isopropoxide species in this temperature range as detected by in situ IR spectroscopy (see Figs. 3 and 6). This is also supported by the in situ Raman spectra during isopropanol oxidation over the supported VS catalyst. The supported VS catalyst exhibited a higher selectivity towards propene formation and the supported VA had a higher selectivity towards acetone at lower isopropanol conversions. These results are quite surprising since propene is known to form on acidic surface sites and the dehydrated supported VA contains much more surface acidic sites that are also stronger acids that the trace surface acidic sites on supported VS [33,34]. If only acidity should be involved, this catalytic observation could show that it is risky to extrapolate from surface acidity measurements under dehydrated conditions to the state of surface acidity under reaction conditions. It would appear

Table 1
IR and Raman assignments of isopropoxides over 10VS and 20VA samples

Assignments [22,41–43]	10VS		20VA	
	IR (cm^{-1})	Raman (cm^{-1})	IR (cm^{-1})	Raman (cm^{-1})
$\nu_{a\text{-}CH_3}$	2978	2968	2974	n.d.
$\nu_{s\text{-}CH_3}$	2938	2926	2935	n.d.
$\nu_{s\text{-}CH_3}$	2921 (shoulder)	2915 (shoulder)	2920 (shoulder)	n.d.
$2\delta_{s\text{-}CH_3}$	2899	2895 (shoulder)	2899	n.d.
$2\delta_{s\text{-}CH_3}$			2889 (shoulder)	n.d.
ν_{CH}	2875	2866	2873 (shoulder)	n.d.
$\delta_{a\text{-}CH_3}$	1472 (shoulder)	n.a.	1471 (shoulder)	n.d.
$\delta_{a\text{-}CH_3}$	1467	n.a.	1465	n.d.
$\delta_{a\text{-}CH_3}$	1453	n.a.	1454	n.d.
$\delta_{a\text{-}CH_3}$	1446 (shoulder)	n.a.	1445 (shoulder)	n.d.
$\delta_{s\text{-}CH_3}$	1384	n.a.	1383	n.d.
$\delta_{s\text{-}CH_3}$	1370	n.a.	1369	n.d.
γ_{CH}	1329	n.a.	1330	n.d.
$\nu_{CO/CC}$	Masked	1162	1165	n.d.
$\nu_{CO/CC}$	Masked	1125 (shoulder)	1130 (shoulder)	n.d.
$\nu_{CO/CC}$	Masked	1110	1105	n.d.
$\nu_{CO/CC}$	965	965	n.a.	940 (uncertain)

that under the current isopropanol oxidation reaction conditions, the supported VS surface is actually more acidic than the supported VA catalyst. This difference in surface acidity between dehydrated surfaces and surfaces exposed to reaction conditions could be related to the presence of adsorbed moisture that is formed by the isopropanol oxidation reaction. This is supported by the significant reduction in acetone and increase in propene formation over both supported vanadia catalysts as the isopropanol conversion is increased and the amount of moisture present proportionally increases with isopropanol and oxygen conversion. However, it is evident that the balance propene/acetone is also determined by the balance acidity/reducibility of the surface sites. The ability of isopropanol to discriminate between surface acidic and surface redox sites of metal oxides suggests that isopropanol is a more realistic chemical probe under reaction conditions than the conventional chemisorption of bases on dehydrated surfaces that have been exposed to vacuum conditions and probably also contain reduced surface sites.

At low reaction temperatures and isopropanol conversions, the acetone/propylene ratio is higher on supported VA than supported VS (see Figs. 1 and 2). CH_3OH-temperature programmed surface reaction (TPSR) spectroscopy revealed that surface methoxy intermediates are more stable on supported VS than VA catalysts [35]. The same relative reactivity between surface isopropoxide on supported VS and VA would be expected if only redox properties should be relevant, because of the analogous surface intermediates and rate-determining-steps involving breaking of the C–H bonds. However, isopropoxides may eliminate to propene while surface methoxides cannot eliminate but only to be oxidized. Thus, again the balance acidity (elimination) versus redox properties (oxidation) is determinant for isopropoxides evolution.

This is also in agreement with observed temperatures required to achieve 100% isopropanol conversion: ~525 K for VA and 575 K for VS (see Figs. 1 and 2). The greater reactivity of the surface V-isopropoxide intermediates on Al_2O_3 relative to SiO_2 may be related to the higher acetone selectivity at low isopropanol conversions over supported VA compared to supported VS since the primary acetone product may more readily be produced and desorb from the active surface VO_x sites on present for supported VA than supported VS.

Surface isopropoxide species have also been proposed as surface reaction intermediates during propane oxidative dehydrogenation reaction to propylene over supported vanadia catalysts [36,37]. Whereas surface isopropoxide is an abundant surface reactive intermediate during isopropanol oxidation at milder reaction temperatures, it is too reactive a surface intermediate to be determined at the temperatures typically employed to activate the more stable propane molecule (573 K and higher). The major propane ODH products are propylene and CO_x, but small amounts of oxygenates can also be present (e.g., acrolein, acrylic acid and isopropanol) [1,19,38,39]. These oxygenates are, however, also observed during propene oxidation over supported vanadia catalysts. In particular, isopropanol can be obtained by rehydration of propene, which prevents the possibility of using this datum as an evidence of the presence of reactive surface isoproxide intermediates during propane ODH [40]. The lack of detection of acetone during propane ODH (in contrast to what happens upon isopropanol ODH, is easily justified by the fact that at such reaction temperatures it is rapidly overoxidized to CO_2. On the other hand the presence of surface acetone from propane, and of alkoxides from isobutane on the surface of very active oxide catalysts are well detectable by IR spectroscopy [36]. In practice, the parallelism between the propene/acetone product ratio upon isopropanol ODH and of propene/CO_x product ratio upon propane ODH over VS and VA, together with the analysis of the surface chemistry of alkoxide intermediates can be taken as a support to the role of isopropoxides as intermediates of both reactions.

5. Conclusions

In summary, this study demonstrates that combining in situ IR, Raman and UV–vis–NIR optical spectroscopic methods collectively provide important molecular level information that allows a better fundamental understanding of the structural nature of the active surface sites, their oxidation states, surface reaction intermediates and surface intermediates–active surface sites interactions during oxidative dehydrogenation reactions. Such fundamental information is necessary for the establishment of molecular structure–reactivity/selectivity models during oxidative dehydrogenation reactions.

Acknowledgment

The work at Lehigh University was supported by the U.S. Department of Energy, Basic Energy Sciences, Grant DE-FG02-93ER14350. C.R. acknowledges a grant from UNIGE.

Reference

[1] P. Arpentinier, F. Cavani, F. Trifirò, The Technology of Catalytic Oxidations, Technip, Paris, 2001.
[2] Levenspiel, Chemical Reaction Engineering, 3rd ed. Wiley, 1999.
[3] L. Cairati, L. Di Flore, P. Forzatti, I. Pasquon, F. Trifiro, Ind. Eng. Chem. Proc. Des. Dev. 19 (1980) 561.
[4] G. Busca, G. Centi, F. Trifirò, J. Am. Chem. Soc. 107 (1985) 7757.
[5] G. Centi, F. Trifirò, J.R. Ebner, V.M. Franchetti, Chem. Rev. 88 (1988) 55.
[6] G. Centi, R.K. Grasselli, F. Trifirò, Catal. Today 13 (1992) 661.
[7] G.A. Somorjai, M. Yang, Top. Catal. 24 (2003) 61.
[8] J.B. Peri, Catalysis Science and Technology, vol. 5, Springer-Verlag, Berlin, Heidelberg, 1984, p. 171.
[9] G. Busca, Catal. Today 27 (1996) 457.
[10] I.E. Wachs, Catal. Today 27 (1996) 437.
[11] G. Busca, J. Raman Spectrosc. 33 (2002) 348.
[12] M.A. Banares, I.E. Wachs, J. Raman Spectrosc. 33 (2002) 359.
[13] L.J. Burcham, G. Deo, X. Gao, I.E. Wachs, Top. Catal. 11 (2000) 85.
[14] A. Gervasini, J. Fenyvesi, A. Auroux, Catal. Lett. 43 (1997) 219.
[15] D. Haffad, A. Chambellan, J.C. Lavalley, J. Catal. Mol. A 168 (2001) 153.
[16] A. Christodoulakis, M. Machli, A.A. Lemonidou, S. Boghosian, J. Catal. 222 (2004) 293.
[17] D. Kulkarni, I.E. Wachs, Appl. Catal. A 237 (2002) 121.
[18] M. Panizza, C. Resini, F. Raccoli, G. Busca, R. Catani, S. Rossini, Chem. Eng. J. 93 (2003) 181.
[19] C. Resini, M. Panizza, L. Arrighi, S. Sechi, G. Busca, R. Miglio, S. Rossini, Chem. Eng. J. 89 (2002) 75.
[20] S. Albonetti, F. Cavani, F. Trifirò, Catal. Rev. Sci. Eng. 38 (1996) 413.
[21] G. Busca, J.C. Lavalley, Spectrochim. Acta A 42 (1986) 443.
[22] P.F. Rossi, G. Busca, V. Lorenzelli, O. Saur, J.C. Lavalley, Langmuir 3 (1987) 52.
[23] V. Sanchez Escribano, G. Busca, V. Lorenzelli, J. Phys. Chem. 94 (1990) 8939.
[24] G. Busca, J. Mol. Catal. 50 (1989) 241.
[25] M.A. Larrubia, G. Busca, Mater. Chem. Phys. 72 (2001) 337.
[26] M.A. Bañares, M.V. Martínez-Huerta, X. Gao, J.L.G. Fierro, I.E. Wachs, Catal. Today 61 (2000) 295.
[27] H. Praliaud, M.V. Mathieu, J. de Chimie Physique 73 (1976) 689.
[28] X. Gao, S.R. Bare, B.M. Weckhuysen, I.E. Wachs, J. Phys. Chem. B 102 (1998) 10842.
[29] X. Gao, I.E. Wachs, J. Phys. Chem. B 104 (2000) 1261.
[30] G. Ramis, C. Cristiani, P. Forzatti, G. Busca, J. Catal. 124 (1990) 574.
[31] I.E. Wachs, J. Catal. 124 (1990) 570.
[32] H. Eckert, I.E. Wachs, J. Phys. Chem. 93 (1989) 6796.
[33] A.M. Turek, E. DeCanio, I.E. Wachs, J. Phys. Chem. 95 (1992) 5008.
[34] I.E. Wachs, G. Deo, B.M. Weckhuysen, A. Andreini, M.A. Vuurman, M. de Boer, M.D. Amiridis, J. Catal. 161 (1996) 211.
[35] X. Wang, I.E. Wachs, Catal. Today 96 (2004) 211.
[36] E. Finocchio, G. Busca, V. Lorenzelli, R.J. Willey, J. Catal. 151 (1995) 204.
[37] K. Chen, A.T. Bell, E. Iglesia, J. Catal. 209 (2002) 35.
[38] C. Resini, M. Panizza, F. Raccoli, M. Fadda, M.M. Carnasciali, G. Busca, E. Fernandez Lopez, V. Sanchez Escribano, Appl. Catal. A 251 (2003) 29.
[39] X. Gao, J.M. Jehng, I.E. Wachs, J. Catal. 209 (2002) 43.
[40] C. Zhao, I.E. Wachs, in press.
[41] P.J. Krueger, J. Jan, H. Wieser, J. Mol. Struct. 5 (1970) 375.
[42] C. Tanaka, Nippon Kagaku Zasshi 83 (1962) 661.
[43] J.H.S. Green, Trans. Faraday Soc. 59 (1963) 1159.